Ballistic spin injection from Fe into ZnSe(001), (111), and (110), and into GaAs(001)

2004 J. Phys.: Condens. Matter 16 4643

(http://iopscience.iop.org/0953-8984/16/26/001)

INSTITUTE OF PHYSICS PUBLISHING JOURNAL OF PHYSICS: CONDENSED MATTER

J. Phys.: Condens. Matter **16** (2004) 4643–4659 PII: S0953-8984(04)77026-5

Ballistic spin injection from Fe into ZnSe(001), (111), and (110), and into GaAs(001)

O Wunnicke, Ph Mavropoulos, R Zeller and P H Dederichs

Institut für Festkörperforschung, Forschungszentrum Jülich, D-52425 Jülich, Germany

E-mail: ph.mavropoulos@fz-juelich.de

Received 27 February 2004
Published 18 June 2004
Online at stacks.iop.org/JPhysCM/16/4643
doi:10.1088/0953-8984/16/26/001

Abstract

We present first-principles calculations of ballistic spin injection in Fe/GaAs and Fe/ZnSe junctions with orientations (001), (111), and (110). We find that the symmetry mismatch of the Fe minority spin states with the semiconductor conduction states can lead to extremely high spin polarization of the current through the (001) interface for hot and thermal injection processes. Such a symmetry mismatch does not exist for the (111) and (110) interfaces, where smaller spin injection efficiencies are found. The presence of interface states at the Fermi energy is found to lower the current spin polarization.

1. Introduction

The idea of exploiting both the charge and the spin of an electron in semiconductor (SC) devices has led to the growing field of spintronics [1]. Several spintronic devices have already been proposed [2, 3], but the full potential of spintronics has still to be discovered. At the moment the essential ingredients of spintronics, e.g., the injection and detection of a spin polarized current, the spin transport in SC, are only partially achieved in experiments. In this paper we wish to investigate one of these main challenges: how to create a spin polarized current in a non-magnetic SC. A very promising approach is via the injection from a common ferromagnetic metal, such as Fe, into a SC due to the high Curie temperature T_C. In this case it has been shown [4] that in the diffusive limit the spin polarization of the injected current is vanishingly small [5, 3, 6], if the contact between the FM and the SC is ohmic. This 'fundamental obstacle' is traced back to the conductivity mismatch between the two materials. It can be overcome by either a ferromagnet with nearly 100% spin polarization at the Fermi energy, e.g., a half-metal, or by inserting a spin polarized interface resistance at the FM/SC interface [7, 8], e.g., an extrinsic tunnelling barrier or an intrinsic Schottky barrier. By means of a Schottky barrier [9–11] or of an Al_2O_3 barrier [12] spin injection could be achieved in experiments.

Here we investigate the spin injection from a ferromagnet (FM) into a SC in the ballistic regime, i.e., the limit where inelastic and incoherent scattering events are negligible. In this case there is no scattering in the perfect bulk regions and the whole resistance results only from the interface region so there is no conductivity mismatch. Therefore other effects emerge that are not present in the diffusive limit: Kirczenow [13] has shown that some FM/SC interfaces can act as ideal spin filter. This is the case if for a direct-gap SC the Fermi surface of the FM projected onto the two-dimensional Brillouin zone has a hole at the $\overline{\Gamma}$ point for one spin direction. But the material combinations Fe/ZnSe and Fe/GaAs investigated here do not fulfil this condition. It has been pointed out that the symmetry of the FM wavefunctions is very important for the spin injection process [14–17]. Where there is a second FM lead for detecting the spin polarization of the current, additional effects such as the forming of quantum well states, Fabry–Perot like resonances and extremely high magnetoresistance ratios have been reported [15].

There are two types of calculation for ballistic spin injection already published: by means of analytical models using plane waves [18–20] and by *ab initio* methods [14–17]. While the model calculations obtain only a few per cent of spin polarization, the inclusion of the full band structure of the FM and the interface region in *ab initio* methods can result in spin polarizations up to 99%. The origin of this high polarization is the difference in symmetry of the Fe d states at the Fermi energy for the majority and the minority spin.

Here we extend our previous work [14, 15] and show more details of the spin injection process. In section 2 the details of the calculations and the Fe/SC systems investigated are given. In section 3 the ballistic spin injection of hot electrons for the Fe/SC(001), (111), and (110) interfaces is investigated. It emerges that the (111) and (110) orientations do not show a large symmetry enforced spin polarization as the (001) orientation does. In section 4 we report on injection of thermal electrons with and without a Schottky barrier, addressing also the effect of resonant interface states. The paper closes with a summary of the results in section 5.

2. Calculation details

The heterostructures investigated consist of a half-space of ideal bulk Fe and one of the ideal bulk SC (either ZnSe or GaAs). Their properties are described by the surface Green function determined by the decimation technique [21]. Between the half-spaces there are several monolayers (MLs) of the interface region, where the atomic potentials are allowed to deviate from their bulk values. This interface region consists of four MLs of Fe and two MLs of SC for the (001) orientation and appropriate numbers of MLs for the (111) and (110) orientations. The corresponding potentials are obtained self-consistently from a Fe/SC/Fe junction geometry by the screened Korringa–Kohn–Rostoker (KKR) Green function method [22, 23]. It is assumed that the SC lattice is matched to the bulk Fe, resulting in an fcc SC lattice constant double the lattice constant of bcc Fe $d_{\mathrm{SC}} = 2d_{\mathrm{Fe}} = 5.742$ Å. The experimental lattice constant of Fe is used. This means that the SC is stretched compared to the bulk lattice constant by 1.3% and 1.6% for ZnSe and GaAs, respectively, resulting in a slightly smaller energy gap. In order to describe the SC accurately, two empty spheres per unit cell are introduced to account for the open space in the geometry of the zinc-blende structure. A perfect two-dimensional translation symmetry in the whole system is assumed and so the in-plane component $\mathbf{k}_{\parallel}$ of the $\mathbf{k}$ vector is conserved while crossing the interface. Then $\mathbf{k}_{\parallel}$ belongs to the common two-dimensional Brillouin zone (2DBZ). The z axis is always assumed to be the growth direction, i.e., standing perpendicular on the interface. Also the conductance G is calculated by a two-dimensional Fourier transformation depending on $\mathbf{k}_{\parallel}$.

The calculations of the ground state properties are performed within the density functional theory in the local density approximation (LDA) for the exchange and correlation terms. It is

well known that it underestimates the energy gap in SC by around one half. Otherwise it gives very accurate FM and SC bands and is well suited for the problem considered. The potentials are described within the atomic sphere approximation, and the wavefunctions are expanded in angular momentum up to a cut-off of $\ell_{\max} = 2$ for self-consistency and $\ell_{\max} = 3$ for the conductance calculations. Spin–orbit coupling and spin-flip scattering are not included in the calculations.

The conductance G is calculated using the Landauer formula [24]. G is expressed as a sum of the transmission probabilities through the scattering region (here the Fe/SC interface) over all available conducting channels. These channels are enumerated by the spin orientation $\sigma = \uparrow$ or $\downarrow$, the bands ν, ν' at the Fermi energy of the left and right lead, respectively, and the $\mathbf{k}_\parallel$ vector. The spin dependent conductance, normalized to the area of the two-dimensional unit cell, reads

$$G^\sigma(E_\mathrm{F}) = \frac{e^2}{h}\frac{1}{A_{\mathrm{2DBZ}}}\sum_{\nu,\nu'}\int_{\mathrm{2DBZ}} \mathrm{d}^2k_\parallel\, T^\sigma_{\nu,\nu'}(\mathbf{k}_\parallel; E_\mathrm{F}) \tag{1}$$

with A_{2DBZ} the area of the 2DBZ. Here, $T^\sigma_{\nu,\nu'}(\mathbf{k}_\parallel; E_\mathrm{F})$ is the probability of transmission from an incoming channel $(\mathbf{k}_\parallel, \nu', \sigma)$ of one lead (Fe) into the outgoing channel $(\mathbf{k}_\parallel, \nu, \sigma)$ of the other lead (SC) at the Fermi level E_F. More generally, we will explore the transmission also at energies higher than E_F. Since the $\mathbf{k}_\parallel$ vector and the spin σ of the electron are conserved in our calculation, they are the same for the incoming and the outgoing states. Here the Landauer formula is evaluated using a Green function formalism introduced by Baranger and Stone [25]. Details of the implementation of the Landauer formula in the KKR Green function formalism are presented elsewhere [26]. The spin polarization P of the current is defined by the spin dependent conductances in both spin bands:

$$P = \frac{G^\uparrow - G^\downarrow}{G^\uparrow + G^\downarrow}, \tag{2}$$

where $G^\uparrow$ and $G^\downarrow$ are the conductances of the majority and the minority spin electrons, respectively.

3. The hot electron injection process

To investigate the effects of the symmetry of the Fe bands, we make calculations first for the hot injection of electrons, i.e., of Fe electrons well above the Fermi level E_F, which falls in the gap of the SC. For most of the calculations we restrict the discussion to the $\overline{\Gamma}$ ($\mathbf{k}_\parallel = 0$) point for simplicity, i.e., we consider only electrons with perpendicular incidence on the interface. This is motivated by the fact that in most spin injection experiments the Fermi energy in the SC is only some tens of millielectronvolts above the conduction band minimum resulting in a very small Fermi sphere around the Γ point. Then, as we shall see, the symmetry of the wavefunctions can assist an extremely high spin polarization of the current.

However, for hot injection at higher energies, one must take more $\mathbf{k}_\parallel$ into account. This procedure is presented in section 3.4. For such cases the restriction to $\mathbf{k}_\parallel = 0$ in sections 3.1–3.3 serves only as a means of understanding the role of the wavefunction symmetry when considering the thermal injection close to E_F, for which only $\mathbf{k}_\parallel \simeq 0$ matters.

3.1. The Fe/SC(001) orientation

First we investigate the spin injection in Fe/SC junctions grown in the (001) orientation. The (001) direction has the highest symmetry and is therefore the best candidate for showing a *symmetry enforced high spin polarization* of the injected current [14], i.e., almost total

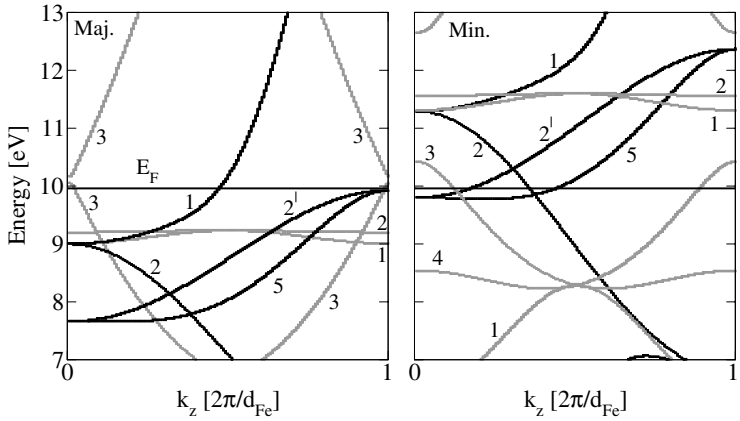

Figure 1. The band structure of Fe(001) at the $\overline{\Gamma}$ point of the 2DBZ (the black curves represent the bulk Γ–H bands and the grey curves the backfolded N–P–N bands). The left panel shows the majority and the right one the minority spin band structure. The Fermi energy is shown by a horizontal line. The numbers denote the symmetries of the bands along the Δ direction (Γ–H) and the D direction (N–P–N) [27].

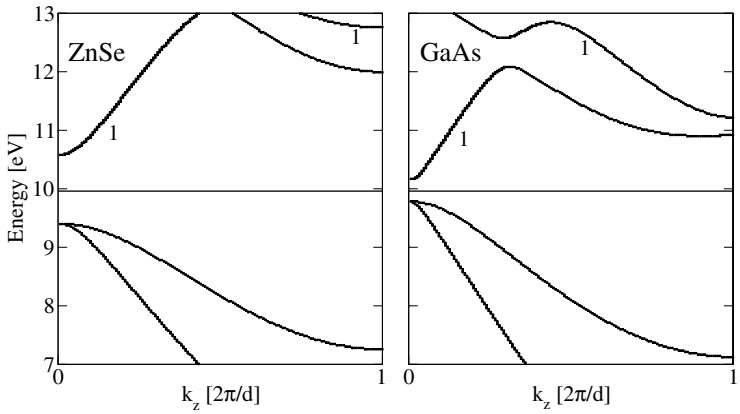

Figure 2. The band structure at the $\overline{\Gamma}$ point of the 2DBZ for ZnSe(001) (left panel) and GaAs(001) (right panel). The numbers denote the symmetries of the bands along the Δ direction [28]. *d* is the SC lattice constant.

reflection of the Fe minority electrons occurs due to the symmetry mismatch between the SC and minority spin Fe bands.

For the investigation of the bands that are available in Fe and in the SC at the $\overline{\Gamma}$ point, it is important to note that the in-plane common two-dimensional unit cell is double in area that of bulk bcc Fe, and the common 2DBZ has half the area of that of bulk bcc Fe. Thus additional Fe bands are backfolded into the 2DBZ and the number of bands at $\overline{\Gamma}$ increases. A description of the backfolding is given in the appendix.

The Fe band structure at the $\overline{\Gamma}$ point along k_z (Γ–H, i.e. the Δ direction), including the backfolded bands, is shown in figure 1 for both spin orientations. This direction has in bulk Fe a C_{4v} symmetry, just like the Fe(001) surface. In the 2DBZ of the SC no bands are backfolded to the $\overline{\Gamma}$ point. The ZnSe and GaAs band structures along Γ–X (the Δ direction) are shown in figure 2. In the SC this direction has a C_{2v} symmetry (a subgroup of C_{4v}), as does the SC(001) surface. Therefore the Fe/SC(001) interface also has the reduced C_{2v} symmetry. As a result,

Table 1. Symmetry properties of energy bands in Fe [001] (C_{4v} symmetry group) and their local orbital analysis. The backfolded bands are indicated by (backf.). The last column shows the coupling to the SC Δ_1 conduction band (C_{2v} symmetry group) based on symmetry compatibility relations and the local orbital form (d orbitals are localized and expected to couple poorly; p_z orbitals extend into the SC and are expected to couple well).

Rep. in Fe	Orbital analysis	Coupling to SC Δ_1
Δ_1	s; p_z; d_{z^2}	Good
$\Delta_{2'}$	d_{xy}	Poor
Δ_2	$d_{x^2-y^2}$	None (orthogonal)
Δ_5	p_x; p_y; d_{xz}; d_{yz}	None (orthogonal)
D_1 (backf.)	s; p_x; d_{yz}; $d_{x^2-y^2} - d_{z^2}$	Poor
D_2 (backf.)	$d_{x^2-y^2} + d_{z^2}$	Poor
D_3 (backf.)	$p_y + p_z$; $d_{xy} + d_{zx}$	Poor

some Fe d bands that are mutually orthogonal in the bulk are able to couple to each other at the interface.

Now it is important to examine which bands of Fe are allowed to couple to the Δ_1 conduction band of the SC which transforms fully symmetrically under the rotations of C_{2v}; this can be found by means of the compatibility relations between the groups C_{4v} and C_{2v}. Note that the symmetry notation that we use for Fe and the SC refers to the different groups, C_{4v} for Fe and C_{2v} for the SC. At E_F and above, the available Fe bands along the Δ direction (black curves in figure 1) and their symmetry and coupling properties are given in table 1. Practically, the only ones that are able to couple well are the Δ_1 bands containing the extended s and p_z orbitals, as well as the d_{z^2} orbitals pointing into the SC, while the $\Delta_{2'}$ bands couple only poorly because they consist of more localized d_{xy} orbitals pointing in-plane. At E_F, and up to 1.2 eV above, the former bands exist only for majority spin electrons, and this is critical for spin injection, to the discussion of which we turn now.

In figure 3 the calculated conductance for the hot injection process for Fe/ZnSe(001) and in figure 4 that for Fe/GaAs(001) are shown. In (a) the Zn and Ga terminated and in (c) the Se and As terminated interfaces are shown. The intermixed interfaces (b) will be discussed later. As is discussed above, the coupling of the minority $\Delta_{2'}$ band to the Δ_1 conduction band of the SC is much weaker than the coupling of the majority spin Δ_1 band. Thus the $\Delta_{2'}$ states are nearly totally reflected at the interface. This results for all three terminations in a very high, symmetry enforced, spin polarization. Around 1.2 eV above the Fermi energy (at 11.3 eV) a Δ_1 band is also available in the minority channel. At this energy the conductance in the minority channel rises drastically, showing that the high spin polarization at lower energies originates precisely from the absence of the Δ_1 Fe band in the minority channel. Also the flat backfolded bands of D_1 and D_2 symmetries give a small contribution to the conductance in the small energy window of around 0.3 eV width, centred around 11.4 eV. At these energies in the ZnSe half-space there is only one conduction band available at the $\overline{\Gamma}$ point, limiting the maximum conductance to one conductance quantum, i.e., 1 e^2/h (per spin per two-dimensional surface unit cell). In the case of the GaAs half-space there are three conduction bands for energies higher than 10.9 eV and so the conductance can rise above 1. The presence of more than one outgoing channel within the same band, occurring in GaAs above 10.9 eV, results also in the interference like oscillations seen in figure 4 at these energies.

Moreover, the conductance can be seen to decrease for small conduction band energies in the SC. This can be explained qualitatively by the vanishing group velocity, such that no current can be transported away from the interface.

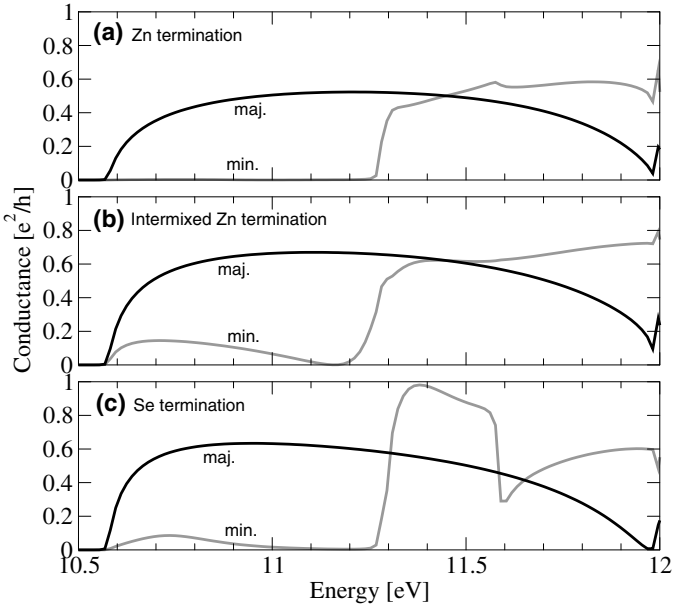

Figure 3. Hot injection of electrons in Fe/ZnSe(001) with a Zn terminated (a), an intermixed Zn terminated (b), and a Se terminated (c) interface. The black curve shows the majority and the grey curve the minority spin. The conductance is evaluated at the $\overline{\Gamma}$ point for simplicity.

3.2. The Fe/SC(111) interface

In this section the spin injection for the Fe/SC junctions grown in the (111) orientation is investigated. In the Fe half-space the [111] direction has a hexagonal symmetry with one atom per unit cell. But in the SC half-space this direction has only a threefold rotational axis. In each ML there is either a cation or an anion (or one of the two types of empty sphere). Also there are a two kinds of possible geometric terminations: one where the terminated SC atom is singly and one where it is triply coordinated to the Fe atoms.

In the SC(111) 2DBZ no bands are backfolded to the $\overline{\Gamma}$ point and the only available band corresponds to the bulk band along the Γ–L high symmetry line. In figure 5 the band structure of Fe(111) at the $\overline{\Gamma}$ point is shown. The band structure shows important differences compared to the (001) orientation: at the Fermi energy in both spin channels there are bands with the same Λ_1 symmetry and therefore the spin polarization is not enforced by symmetry. All differences obtained in the conductances for both spin directions are due to the different couplings of the Fe bands to the SC.

The calculated results for the hot injection process in Fe/ZnSe(111) with a Zn terminated interface are shown in figure 6 for both the cases of singly and triply coordinated Zn interface atoms. Also, for this orientation, the conductance is shown at the $\overline{\Gamma}$ point as before. For both the singly and the triply coordinated Zn terminations the spin polarization is much smaller than for the (001) interface, demonstrating the lack of a symmetry enforced spin filtering. Above 12.0 eV no bands exist in ZnSe at the $\overline{\Gamma}$ point in the [111] direction, and so no propagating states are available.

3.3. The Fe/SC(110) interface

This section deals with Fe/SC(110) oriented junction. This is the one with the lowest symmetry considered in this work, and a symmetry enforced spin polarization does not occur.

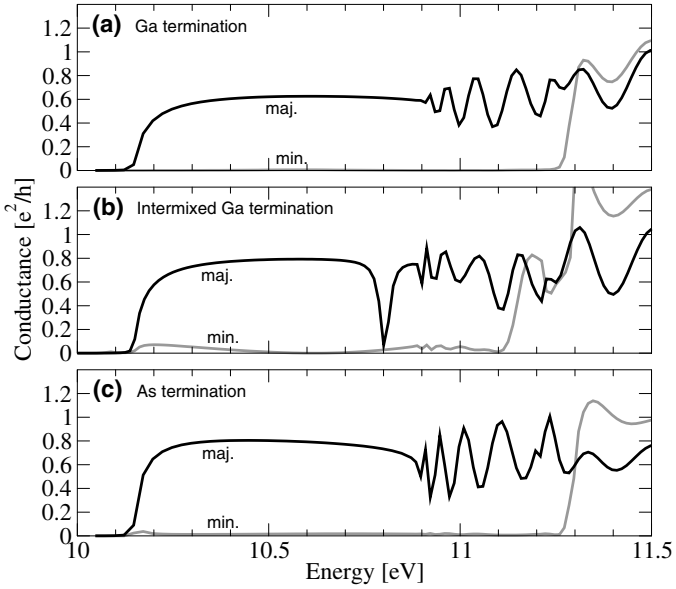

Figure 4. As figure 3, but for Fe/GaAs(001) with a Ga terminated (a), an intermixed Ga terminated (b), and an As terminated interface (c). Black curves refer to majority and grey curves to minority spin directions.

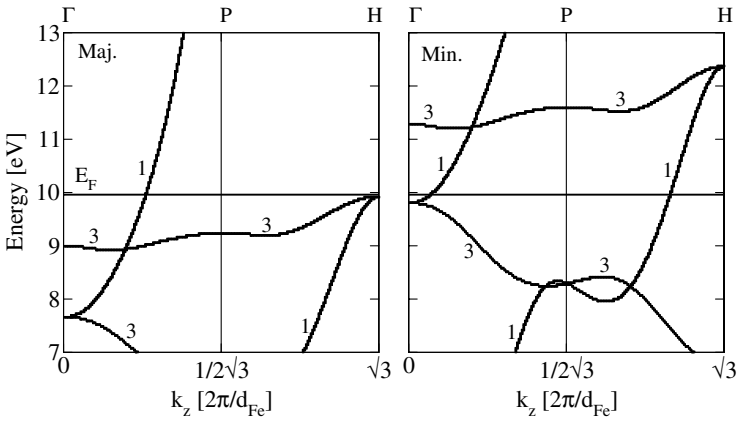

Figure 5. The band structure of Fe(111) at the $\overline{\Gamma}$ point of the 2DBZ (corresponding to the bulk band along the Γ–P–H symmetry line). The left panel shows the majority and the right panel the minority spin. The Fermi energy is shown by a horizontal line. The numbers denote the symmetry of the corresponding Λ (between Γ and P) and F (between P and H) symmetry directions [27].

Furthermore, the surface unit cell in the SC half-space contains all four kinds of atoms (cations, anions, and both kinds of vacancies) and is larger than the (001) and the (111) unit cells. Matching the two-dimensional translational symmetry, the Fe surface unit cell also has to contain four Fe atoms. This results in a very small 2DBZ for this orientation, leading even in the SC half-space to backfolded bands at the $\overline{\Gamma}$ point. The band structure of Fe(110) at the $\overline{\Gamma}$ point with the different backfolded bands is shown in figure 7. In the SC(110) half-space there are two bands available at the $\overline{\Gamma}$ point due to backfolding. Because of this the maximum conductance per spin direction is $2\ e^2/h$.

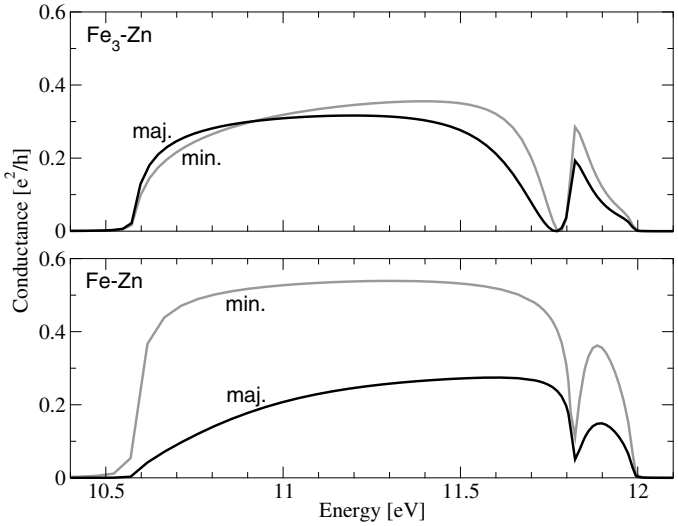

Figure 6. Hot injection of electrons in Fe/ZnSe(111) for a Zn terminated interface, where the Zn atoms are either triply coordinated (upper plot) or singly coordinated (lower plot) with respect to the interface Fe atoms. The black curves refer to the majority and the grey curves the minority spin direction. The conductance is evaluated at the $\overline{\Gamma}$ point for simplicity.

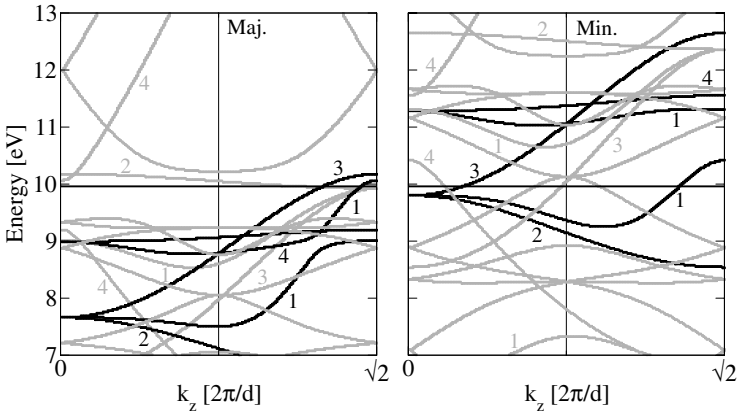

Figure 7. The band structure of Fe(110) at the $\overline{\Gamma}$ point of the 2DBZ. The backfolded bands are shown in grey, and those for the Γ–N direction in black. The left plot shows the majority and the right plot the minority spin states. The Fermi energy is shown by a horizontal line. The numbers give the symmetries of the corresponding bulk bands [27], where possible.

The variety of backfolded bands and the reduced symmetry of the [110] direction do not allow a simple symmetry-based discussion and the spin polarization is not enforced by symmetry. This is also shown in figure 8, where the conductance at the $\overline{\Gamma}$ point for the hot injection process is presented.

From the above we conclude that the only candidate for showing a symmetry enforced high current spin polarization is the (001) interface. Thus, in what follows, we restrict our study to this orientation.

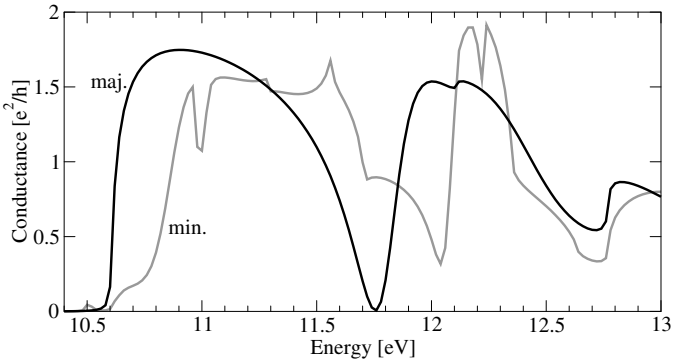

Figure 8. Hot injection of electrons in Fe/ZnSe(110). The black curve shows the majority and the grey curve the minority spin conductance. Since all four different atoms (Zn, Se, and two vacancies) are located in each ML, there is only one possible termination. The conductance is evaluated at the $\overline{\Gamma}$ point for simplicity.

3.4. The hot injection process, $\mathbf{k}_\parallel$ resolved

In the hot injection process the restriction to the $\overline{\Gamma}$ point is motivated by the fact that in most applications the Fermi level is positioned only slightly above the conduction band minimum resulting in a very small Fermi sphere around the Γ point. More correctly the conductance should be integrated over the whole 2DBZ, because states slightly away from the $\overline{\Gamma}$ point are also populated for higher injection energies. Therefore in figure 10 the $\mathbf{k}_\parallel$ resolved conductances are shown for the majority and minority spin electrons for the Zn terminated Fe/ZnSe(001) interface. The energy of the injected electrons is 500 meV above the conduction band minimum E_C. In this case the polarization at the $\overline{\Gamma}$ point is $P_{\overline{\Gamma}} = 99.7\%$. If the conductance is integrated over the 2DBZ the polarization is reduced to $P_{\text{integrated}} = 39.5\%$. The reason is a higher conductance in the minority band for states away from the $\overline{\Gamma}$ point. The symmetry arguments discussed above are valid only at this high symmetry point. For states $\mathbf{k}_\parallel \neq 0$ other Fe minority states are also allowed to couple to the SC Δ_1 conduction band and so the minority conductance rises continuously as we depart from the centre of the 2DBZ. In comparison, for electrons injected at $E_C + 100$ meV, we obtain $P_{\overline{\Gamma}} = 98.4\%$, and a high value of $P_{\text{integrated}} = 97.5\%$. As can be seen from figure 9, $P_{\text{integrated}}$ drops rapidly with increasing injection energy, while $P_{\overline{\Gamma}}$ remains close to 100% and drops (even reversing its sign) only at high energies ($E_C + 1000$ meV), when the minority spin Δ_1 band of Fe is reached. We conclude that the high, symmetry enforced, spin polarization can be realized only for energies up to a few tens of millielectronvolts above the conduction band edge.

In the conductance plot (figure 10) for the minority electrons the reduced C_{2v} symmetry of the Fe/SC(001) interface can be seen directly. The majority spin conductance behaves like free electrons travelling across a potential step and is practically unaffected by the reduced symmetry. The circularly symmetric form of $G^{\uparrow}(\mathbf{k}_\parallel)$ and the twofold-symmetric form of $G^{\downarrow}(\mathbf{k}_\parallel)$ can be understood in terms of the form of the Bloch functions for small deviations from $\mathbf{k}_\parallel = 0$ in the same manner as described in [15] for the Fe/SC/Fe(001) junctions.

3.5. The intermixed interface

By means of an *ab initio* study [29] it has been found that the interface of Fe/GaAs(001) with a Ga terminated interface is energetically more stable, if Fe atoms diffuse into the vacancy

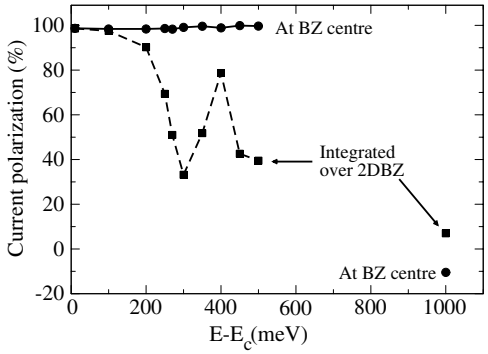

Figure 9. Spin polarization at $\overline{\Gamma}$ (full line) and integrated over the two-dimensional Brillouin zone (dashed line) for several energies of hot injection for the Fe/ZnSe(001) case, Zn terminated.

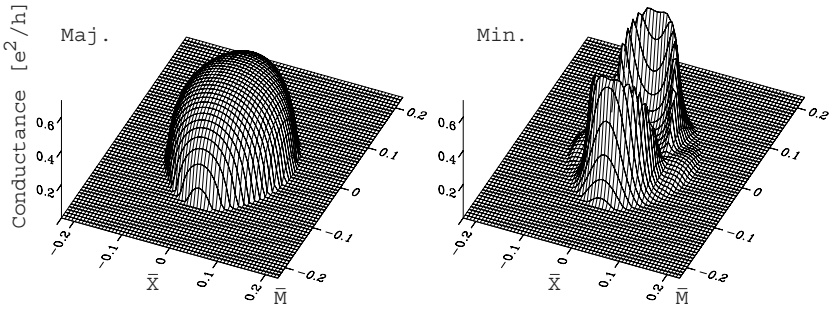

Figure 10. The conductance in the hot injection process in Fe/ZnSe(001) (Zn termination), resolved in $\mathbf{k}_\parallel$. The left plot shows the conductance of the majority and the right one of the minority spins. Only one tenth of the 2DBZ around the $\overline{\Gamma}$ point is shown. The Fermi energy lies 500 meV above the conduction band minimum in the semiconductor half-space. The reciprocal vectors are in units of $2\pi/d_{\mathrm{SC}}$.

sites of the first Ga ML. In the case of an As terminated interface the abrupt interface is found to be more stable than the intermixed one. The former case is accompanied by rather large lattice distortions which are not taken into account in our calculations. Although we do not know of analogous studies for Fe/ZnSe(001) interfaces, we have also calculated the intermixed interface in the case of a Zn termination. This is done by replacing the empty spheres in the first Ga (or Zn) layer by Fe atoms, so that we obtain a 50%–50% intermixed monolayer. The results are shown in figures 3(b) and 4(b) for the hot injection process with an intermixed Zn and Ga interface, respectively. The still high spin injection polarization can be explained by the fact that the intermixed Fe atoms do not change or reduce the C_{2v} symmetry of the interface and so the symmetry arguments are still valid. This is a different effect to the interface roughness that reduces the spin polarization drastically [16, 30]. Solely the couplings of the Fe states to the SC are changed. In both cases the coupling in the minority band is enhanced in comparison to that for the atomically abrupt interfaces shown in figures 3(a) and 4(a).

4. The thermal injection process; the role of resonant interface states

In this section the injection of thermal electrons is investigated. This is achieved by lowering the potentials in the SC half-space by means of a rigid shift, so that the Fermi energy falls

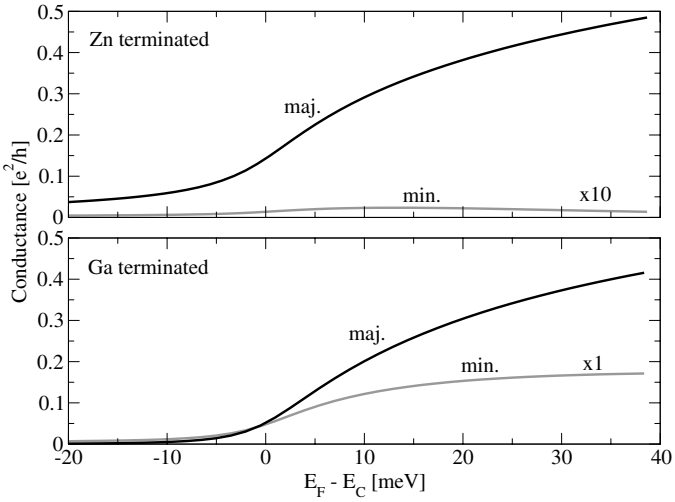

Figure 11. Thermal injection of electrons in Fe/ZnSe (upper plot) and Fe/GaAs(001) (lower plot) with an intermixed Zn and Ga interface, respectively. The black curve shows the majority and the grey curve the minority spin. The conductance is evaluated at the $\overline{\Gamma}$ point. Note that the minority conductance is enlarged by a factor of 10 in the case of the Zn termination.

some tens of millielectronvolts above the conduction band minimum. All other atomic sphere potentials are kept in their ground state position—in particular, also the potentials of the two SC monolayers in the interface region. This shifting simulates the effect of n doping or an applied gate voltage in a field-effect-transistor device. The electrons are injected at the E_{F} of the Fe half-space directly into the conduction band. Since the Fermi energy is only slightly above the conduction band minimum and since the effective masses of ZnSe and GaAs are small, the resulting Fermi wavevector in the SC half-space is very small (around one hundredth of the distance to the boundary of the 2DBZ). Therefore we present here only the conductance for the $\overline{\Gamma}$ point. The polarization evaluated changes only slightly if the conductances are integrated over the whole 2DBZ.

4.1. Thermal injection without a Schottky barrier

The results for Fe/ZnSe and Fe/GaAs(001) are discussed in [14] and show a very high spin polarization of more than 97% for ZnSe and practically 100% for GaAs(001). Similar results are found in Fe/SC/Fe(001) junctions [15]. Here we add thermal injection with an intermixed Zn and Ga terminated interface (figure 11). In the case of an intermixed Zn interface nearly the same conductances are obtained as for the abrupt one (figure 3 in [14]). But a drastic increase of the minority conductance can be seen for the intermixed Ga interface, resulting in a much smaller spin polarization. The reason for this increase is an interface resonance localized at the intermixed Fe atoms. This can be seen in the density of states (DOS) for this heterojunction shown in figure 12 for the intermixed Zn and Ga interfaces. The arrows indicate the position of the Fe resonance. In the case of the intermixed Zn interface this resonance lies slightly above E_{F} and gives rise to the small maximum in the minority conductance at $E_{\mathrm{F}} - E_{\mathrm{C}} = 15$ meV seen in figure 11. In the DOS for the intermixed Ga interface this resonance lies nearly on the Fermi energy, so it has a strong influence on the minority conductance. Since the energy position of this resonance is believed to depend strongly on the interface properties, e.g., lattice

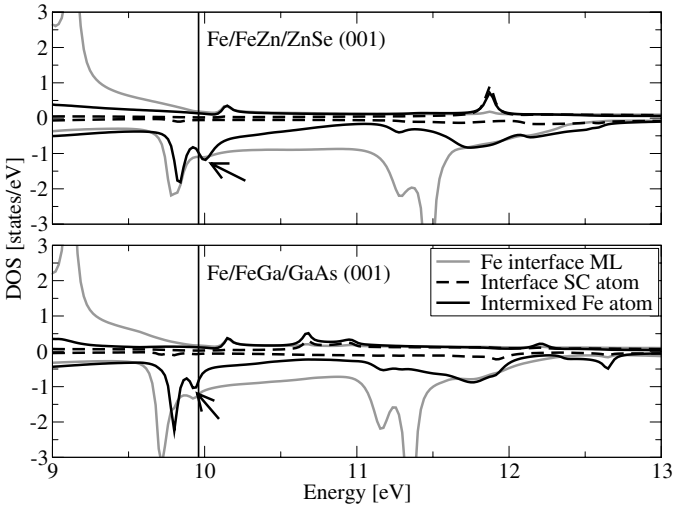

Figure 12. The density of states (DOS) for the thermal injection process in Fe/ZnSe(001) (upper plot) and Fe/GaAs(001) (lower plot) with an intermixed Zn or Ga interface. Arrows indicate the resonance at the intermixed Fe atom. Negative numbers on the DOS axis correspond to minority spin.

relaxations, further investigations are needed for the exact energy position. If the injection process is evaluated at only 0.3 eV higher energies, the influence of this resonance is negligible and the normal high spin polarization is restored in both terminations.

We note that this particular interface state is characteristic for Fe(001). It arises from the breaking of translational symmetry at the (001) interface, leading to a dangling bond state in the s–d hybridization gap of the bulk. Since this state is usually partially occupied, it is pinned at E_F. It then couples to the bulk Bloch functions due to the reduced point group symmetry of the Fe/SC interface (C_{2v} instead of C_{4v}). In analogy, a surface state occurs at the (001) Fe surface [31], but does not couple to the bulk states since the point group symmetry is not reduced. In other interfaces ((111) and (110)) this mechanism does not occur, since no hybridization gap exists at E_F. In this respect, one observes that the mechanism which causes the symmetry enforced spin polarization of the current is also responsible for the interface states: i.e., the Δ_1 gap.

4.2. Thermal injection through a Schottky barrier

In theoretical studies for diffusive transport based on spin accumulation [7, 8] it is shown that the negligible spin polarization due to the conductivity mismatch between the ferromagnetic metal and the semiconductor [4] can be overcome by means of a spin dependent tunnelling barrier at the interface. Such a barrier could be the Schottky barrier created at the interface. Although the approaches in [7, 8, 4] assume diffusive transport, tunnelling barriers can be described in ballistic regime.

Therefore in this section the thermal injection process is extended to the case where a Schottky barrier at the interface is included. The potentials used for these junctions are the same as in the thermal injection process, but with an inserted tunnelling barrier at the interface. The barrier is modelled by a rigid shift of each SC atom potential, constant within each monolayer; the band diagram is shown schematically in figure 13. It starts at the third SC layer

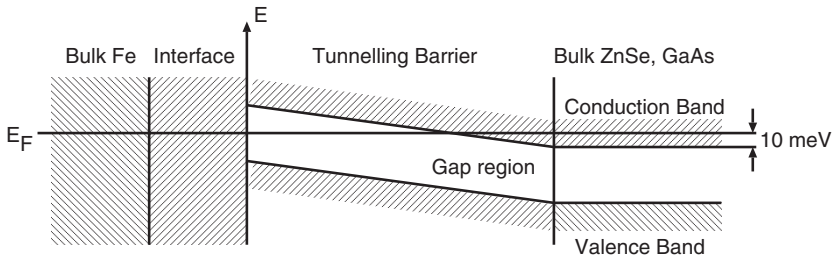

Figure 13. A schematic representation of the bands near the Fe/Semiconductor interface in the presence of a Schottky tunnelling barrier. The electrons are injected at E_F.

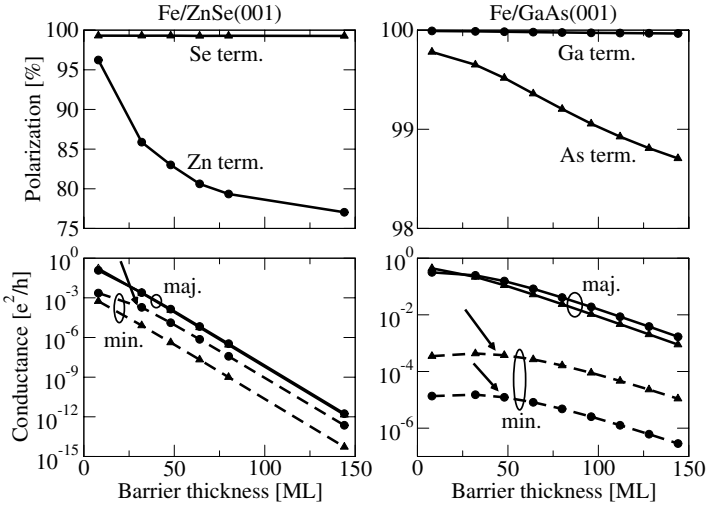

Figure 14. The influence of a smooth Schottky barrier on the spin dependent conductance (lower plots) and the spin polarization (upper plots) for Fe/ZnSe(001) (left panel) and Fe/GaAs(001) (right panel). Circles show the conductance for the Zn or Ga and triangles for the Se or As termination. The conductance is evaluated at the $\overline{\Gamma}$ point. Arrows indicate the influence of the resonant interface state causing a non-exponential decay of the conductance for moderate barrier thickness. In Fe/ZnSe(001) the lines for the majority conductances lie on top of each other.

from the interface, and increases linearly in magnitude with distance from the interface. In this way the SC bands are gradually shifted downward. Finally, at the end of the barrier, E_F lies 10 meV above the conduction band edge (and the shift is not changed from then on), while at the interface E_F lies in the middle of the gap. Several barrier thicknesses are considered, varying between 0 and 140 MLs.

As shown in [14] a tunnelling barrier at the Fe/SC(001) interface also gives a high spin polarization. Only in the case of a resonant interface state near E_F, especially seen in Fe/ZnSe(001) with a Zn terminated interface, is the polarization reduced. Here we will discuss the effect in more detail. In figure 14 the conductance and the polarization depending on the barrier thickness are shown for Fe/ZnSe and Fe/GaAs(001), respectively. Due to the small Fermi wavevector, the conductance is again analysed only at the $\overline{\Gamma}$ point. The polarizations agree with the ones correctly integrated over the 2DBZ within 5%.

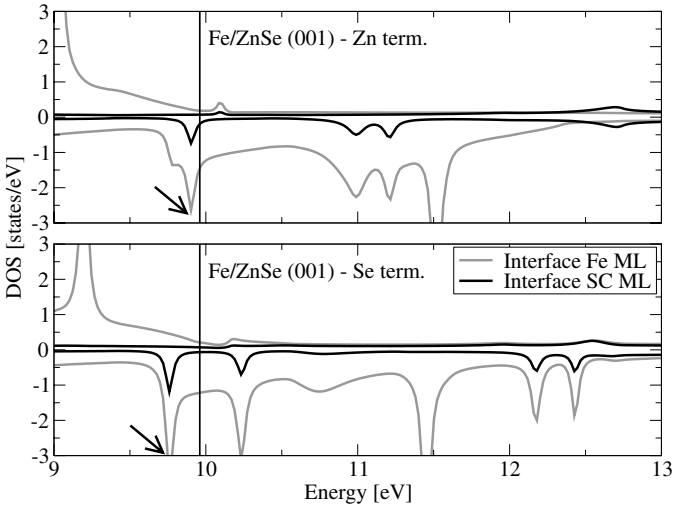

Figure 15. The DOS at the $\overline{\Gamma}$ point for Fe/ZnSe(001) with a Zn (upper plot) and a Se terminated interface (lower plot). Grey lines show the DOS of the Fe interface ML and black lines the DOS of the Zn or Se interface ML. The vertical lines indicate the position of the Fermi energy. All potentials are in the ground state position. Arrows indicate the peak in the DOS due to the resonant interface state.

Except for the Se terminated Fe/ZnSe(001) interface, all terminations show the influence of a resonant interface state in the minority band, resulting in a slightly higher conductance for the minority spins with thicker barriers. This leads to a slight reduction of the spin polarization. For Fe/GaAs(001) this effect is also visible in the conductance but is negligible for the spin polarization due to the much larger difference of the conductances of the spins than in Fe/ZnSe. To facilitate discussing this effect in more detail, in figure 15 the DOS at the $\overline{\Gamma}$ point is shown for Fe/ZnSe(001). The DOS for Fe/GaAs(001) is qualitatively comparable for this purpose. In the DOS an interface state is visible near the Fermi energy in the minority spin channel. This state has Δ_1 symmetry and lies in the energy region of the Δ_1 hybridization gap of the Fe minority band structure. It can penetrate well a Schottky barrier of moderate thickness since the evanescent wave with the longest decay length is of the same Δ_1 symmetry [32]. In the Fe half-space this interface state is normally also evanescent since there are no propagating states that it can couple to. But due to the reduced symmetry of the interface the Δ_1 interface state couples weakly to the Fe $\Delta_{2'}$ band and becomes resonant. In the case of the Se terminated Fe/ZnSe(001) interface the interface state lies further away from E_F and does not contribute to the conductance.

The potentials used for the DOS in figure 15 are the ground state potentials, i.e., E_F is in the middle of the gap in the SC half-space and no Schottky barrier is inserted. If now a Schottky barrier is introduced into the junction, the system and the resonant interface state are slightly distorted, because the Δ_1 interface state interacts with the Δ_1 conduction band of the semiconductor. This results in a slight downshift in energy of the resonant interface state away from E_F for smaller Schottky barriers. The reduction of the spin polarization with thicker Schottky barriers can thus be explained by a shift of the resonant interface state towards E_F.

Furthermore one can estimate the interface resistance under the assumption of diffusive transport in the bulk, using Schep's formula [33, 34]. Although this has been derived for metallic multilayers, we have applied it to this case. Our results are summarized in table 2. More details can be found in [35].

Table 2. The interface resistance R_I and spin polarization P for two Schottky barrier thicknesses and all four terminations in Fe/SC(001). Results are obtained by integration over the whole 2DBZ. A thickness of 80 ML corresponds to 115 Å.

		P (Zn)	P (Se)	P (Ga)	P (As)
R_I (Ω m^2)	(8 ML)	1×10^{-10}	8×10^{-11}	2×10^{-10}	2×10^{-10}
P	(8 ML)	96%	96%	99.8%	99.8%
R_I (Ω m^2)	(80 ML)	5×10^{-5}	7×10^{-5}	2×10^{-9}	4×10^{-9}
P	(80 ML)	77%	97%	99.2%	98.0%

5. Summary and conclusions

We have reported first-principles calculations on spin injection from Fe into GaAs and ZnSe through ideal (001), (111), and (110) interfaces. The electronic transport has been assumed to be in the ballistic regime, and the interfaces have been assumed to have two-dimensional periodicity, so that $\mathbf{k}_\parallel$ is conserved during scattering at the interface. Then, in a Landauer–Büttiker approach, the conductance is determined from the transmission probability summed over all $\mathbf{k}_\parallel$. Under these assumptions, we have considered hot and thermal injection—the latter also in the presence of a Schottky barrier. We have reached the following conclusions.

(i) The spin polarization of the current is highest when most incoming Fe Bloch states of one spin direction are totally reflected due to symmetry mismatch with the SC conduction band states—we call this effect 'symmetry enforced spin polarization'. This is the case for the (001) interface, where minority spin electrons for $\mathbf{k}_\parallel = 0$ practically cannot be transmitted. The lower symmetry of the (111) and (110) interface does not lead to such a selection rule. Even for the (001) interface, in the case of hot injection, above an energy threshold where the Fe minority Δ_1 band starts, the minority spin current increases rapidly even at $\mathbf{k}_\parallel = 0$, being symmetry allowed.

(ii) For the symmetry enforced spin polarization to be realized, the injection must take place close to the conduction band edge, so only states near $\mathbf{k}_\parallel = 0$ are relevant; these have well defined and suitable symmetry properties. Also, the interface should be well ordered; otherwise $\mathbf{k}_\parallel$ is not conserved and incoming minority spin Fe states from all $\mathbf{k}_\parallel$ can scatter into the SC conduction band, leading to a decrease of the spin polarization [16].

(iii) The case of thermal injection (i.e. exactly at E_F), has been considered for the (001) interface with and without a Schottky barrier. The symmetry concepts still hold, since the least-decaying complex band of the tunnelling barrier has the same symmetry properties as the conduction band (both are of Δ_1 character). We have seen that resonant interface states existing in the vicinity E_F for minority spin can be important for the spin polarization of the current. In the case of a Schottky barrier they can provide a resonant tunnelling channel for the minority spin electrons decreasing the spin injection effect. For the cases considered this effect is, however, small.

It can be argued that a well ordered interface, necessary for our symmetry selection rule, is difficult to realize experimentally. However, successful attempts at increasing the spin injection efficiency have been recently reported for Fe/GaAs(001). The increase of the spin polarization to 32% has been attributed to an improvement of the quality of the interface [11]. Therefore, we are optimistic that our work will motivate further research in this direction.

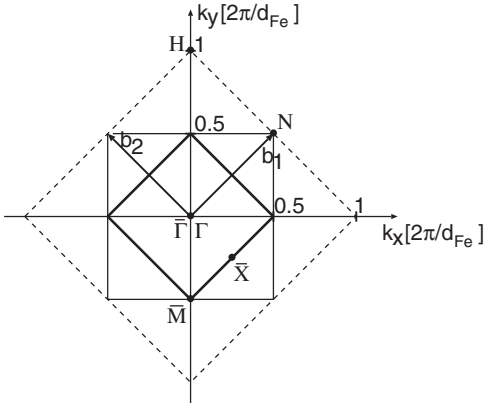

Figure A.1. The 2DBZ for Fe(001) adapted to the Fe/SC(001) interface (thick line). For comparison the 2DBZ for a free Fe(001) surface (thin solid line) and the (001) cut through the bulk Brillouin zone (thin dashed line) are also shown. The k_z vector along the [001] direction varies between $\pm 2\pi/d_{\mathrm{Fe}}$.

Acknowledgments

The authors thank Arne Brataas for helpful comments. This work was supported by the RT Network *Computational Magnetoelectronics* (Contract RTN1-1999-00145) of the European Commission.

Appendix. Geometry of the reduced 2DBZ

Here we discuss briefly the geometry of the 2DBZ and the available bands at the $\overline{\Gamma}$ point for the (001), (111), and (110) orientation in the Fe and the SC half-space. More details can be found elsewhere [17].

First we investigate the backfolded bands for the Fe(001) half-space. In figure A.1 the 2DBZ and the cut perpendicular to the [001] direction of the bulk Brillouin zone (BZ) are shown. At the $\overline{\Gamma}$ point two bands are available. One is a band that is not backfolded, corresponding to the bulk band along Γ–H, i.e., the Δ direction. Also, there is one band that is backfolded, by applying, once, the reciprocal surface lattice vectors $\mathbf{b_1}$ or $\mathbf{b_2}$, corresponding to the bulk band along N–P–N, i.e., the D direction. In the SC half-space no additional bands are backfolded to the $\overline{\Gamma}$ point and the only available band corresponds to the bulk band along Γ–X, i.e., the Δ direction.

Next we discuss the (111) case briefly. As for the (001) orientation, additional bands are obtained by backfolding to the $\overline{\Gamma}$ point due to the large lattice constant in the Fe half-space. The band at the $\overline{\Gamma}$ point that is not backfolded corresponds to the bulk band along the Γ–P–H high symmetry line, because in the 2DBZ the k_z vector extends from $-\sqrt{3}$ to $\sqrt{3}$ in units of $2\pi/d_{\mathrm{Fe}}$. Also one additional band is backfolded to the $\overline{\Gamma}$ point corresponding to the bands of the same Γ–P–H high symmetry line as the band that is not backfolded. In the SC half-space only the band available at the $\overline{\Gamma}$ point corresponds to the bulk band along Γ–L, i.e., the Λ direction.

Due to the much larger surface unit cell of Fe(110) compared to the Fe bulk BZ, four bands are available at the $\overline{\Gamma}$ point. The non-backfolded band corresponds to the Γ-N bulk band (Σ direction). One backfolded band corresponds to the bulk band between N and H, i.e., in the Σ direction. In addition two bands are backfolded to the $\overline{\Gamma}$ point that are *not* along a

high symmetry direction in the Fe bulk BZ. Because of these bands, a symmetry enforced spin polarization cannot be expected for the (110) orientation.

In the (110) orientation, even in the SC 2DBZ, one band is backfolded. The two bands available at the $\overline{\Gamma}$ point correspond to the same bulk band between Γ and K (in the Σ direction). Thus, the maximum possible conductance in the (110) orientation is $2\ e^2/h$ per spin channel.

References

[1] Wolf S A, Awschalom D D, Buhrman R A, Daughton J M, von Molnár S, Roukes M L, Chtchelkanova A Y and Treger D N 2001 *Science* **294** 1488
[2] Datta S and Das B 1990 *Appl. Phys. Lett.* **56** 665
[3] Gardelis S, Smith C G, Barnes C H W, Linfield E H and Ritchie D A 1999 *Phys. Rev.* B **60** 7764
[4] Schmidt G, Ferrand D, Molenkamp L W, Filip A T and van Wees B J 2000 *Phys. Rev.* B **62** R4790
[5] Filip A T, Hoving B H, Jedema F J, van Wees B J, Dutta B and Borghs S 2000 *Phys. Rev.* B **62** 9996
[6] Hammar P R, Bennett B R, Yang M J and Johnson M 1999 *Phys. Rev. Lett.* **83** 203
[7] Rashba E I 2000 *Phys. Rev.* B **62** R16267
[8] Fert A and Jaffrès H 2001 *Phys. Rev.* B **64** 184420
[9] Zhu H J, Ramsteiner M, Kostial H, Wassermeier M, Schönherr H-P and Ploog H H 2001 *Phys. Rev. Lett.* **87** 16601
[10] Hanbicki A T, Jonker B T, Itskos G, Kioseoglou G and Petrou A 2002 *Appl. Phys. Lett.* **80** 1240
[11] Hanbicki A T, van 't Erve O M J, Magno R, Kioseoglou G, Li C H, Jonker B T, Itskos G, Mallory R, Yasar M and Petrou A 2003 *Appl. Phys. Lett.* **82** 4092
[12] Motsnyi V F, Safarov V I, De Boeck J, Das J, van Roy W, Goovaerts E and Borghs G 2002 *Appl. Phys. Lett.* **81** 265
[13] Kirczenow G 2001 *Phys. Rev.* B **63** 54422
[14] Wunnicke O, Mavropoulos Ph, Zeller R, Dederichs P H and Grundler D 2002 *Phys. Rev.* B **65** R241306
[15] Mavropoulos Ph, Wunnicke O and Dederichs P H 2002 *Phys. Rev.* B **66** 024416
[16] Zwierzycki M, Xia K, Kelly P J, Bauer G E W and Turek I 2003 *Phys. Rev.* B **67** 092401
[17] Wunnicke O 2003 *PhD Thesis* RWTH-Aachen
[18] Grundler D 2001 *Phys. Rev.* B **63** R161307
[19] Hu C-M and Matsuyama T 2001 *Phys. Rev. Lett.* **87** 066803
[20] Heersche H B, Schäpers Th, Nitta J and Takayanagi H 2001 *Phys. Rev.* B **64** R161307
[21] Turek I, Drchal V, Kudrnovský J, Ŝob M and Weinberger P 1997 *Electronic Structure of Disordered Alloys, Surfaces, and Interfaces* (Boston, MA: Kluwer–Academic)
[22] Wildberger K, Zeller R and Dederichs P H 1997 *Phys. Rev.* B **55** 10074
[23] Papanikolaou N, Zeller R and Dederichs P H 2002 *J. Phys.: Condens. Matter* **14** 2799
[24] Landauer R 1957 *IBM J. Res. Dev.* **1** 233
[25] Baranger H U and Stone A D 1989 *Phys. Rev.* B **40** 8169
[26] Mavropoulos Ph, Papanikolaou N and Dederichs P H 2004 *Phys. Rev.* B **69** 125104
(Mavropoulos Ph, Papanikolaou N and Dederichs P H 2003 *Preprint* cond-mat/0306604)
[27] Callaway J and Wang C S 1977 *Phys. Rev.* B **16** 2095
[28] Wang C S and Klein B M 1981 *Phys. Rev.* B **24** 3393
[29] Erwin S C, Lee S-H and Scheffler M 2002 *Phys. Rev.* B **65** 205422
[30] Stroud R, Hanbicki A, Park Y, Peukhov A, Jonker B, Itskos G, Kioseoglou G, Furis M and Petrou A 2002 *Phys. Rev. Lett.* **89** 166602
[31] Papanikolaou N, Nonas B, Heinze S, Zeller R and Dederichs P H 2000 *Phys. Rev.* B **62** 11118
[32] Mavropoulos Ph, Papanikolaou N and Dederichs P H 2000 *Phys. Rev. Lett.* **85** 1088
[33] Schep K M, van Hoof J B A N, Kelly P J, Bauer G E W and Inglesfield J E 1997 *Phys. Rev.* B **56** 10805
[34] Stiles M D and Penn D R 2000 *Phys. Rev.* B **61** 3200
[35] Wunnicke O, Mavropoulos Ph and Dederichs P H 2003 *J. Supercond.: Incorporating Novel Magn.* **16** 171